Spin-rectification and electrically controlled spin transport in molecular-ferroelectrics-based spin valves

Yuewei Yin,[1,2] Xuanyuan Jiang,[1] Mark A. Koten,[3] Jeffrey E. Shield,[3]
Xuegang Chen,[1] Yu Yun,[1] Alpha T. NDiaye,[4] Xia Hong,[1] and Xiaoshan Xu[1]

[1]*Department of Physics and Astronomy, Nebraska Center for Materials and Nanoscience, University of Nebraska, Lincoln, Nebraska 68588, USA.*
[2]*Hefei National Laboratory for Physical Sciences at the Microscale, Department of Physics, and CAS key Laboratory of Strongly-Coupled Quantum Matter Physics, University of Science and Technology of China, Hefei, China.*
[3]*Department of Mechanical and Materials Engineering, University of Nebraska, Lincoln, Nebraska 68588, USA.*
[4]*Advanced Light Source, Lawrence Berkeley National Laboratory, Berkeley, California 94720, USA.*

(Dated: April 18, 2020)

We report a spin-rectification effect in a spin valve structure consisting of ferroelectric croconic acid ($C_5H_2O_5$) sandwiched between ferromagnetic electrodes $La_{0.7}Sr_{0.3}MnO_3$ and Co, which can be switched between a high-resistance (OFF) and a low-resistance (ON) states by a poling voltage. In the OFF state the magnetoresistance (MR) sign reverses with the measurement voltage with a 0.1 V offset, suggesting a spin-rectification behavior, while in the ON state MR remains negative. These observations can be understood in terms of electrically-controlled interfacial energy-band alignment either from the electrostatic effect or from the interfacial redox process. The observed spin-rectification effect suggests the possibility of diode-like devices for spin-polarized current.

Electrical control of spin transport is critical for developing spin-based circuitry[1–3]. The realization of this control hinges on the sensitivity of fundamental processes such as generation and detection of spin currents to the electrical field. In multilayer structures such as spin valves, spin current can be generated and detected using ferromagnet (FM)/non-magnet (NM) interfaces. Their efficiencies are determined by the interfacial spin polarizations P^s, which manifest in magnetoresistance (MR)[4]. Therefore, manipulation of P^s can be an effective way for electrical control of spin transport.

A significant change of P^s is its sign reversal. Reversal of P^s sign when the electrical current is reversed, can be viewed as a spin-rectification effect for the FM/NM interface, which could be useful for tunable spin-filtering. Spin-rectification of an FM/NM interface in a spin valve structure can be inferred from an MR sign reversal with measurement voltage, if the P^s sign of the other FM/NM interface is unchanged, as illustrated in Fig. 1(a). Although the magnitude of MR naturally decreases with the measurement voltage[5–11]due to, e.g., spin depolarization of hot carries[12], MR sign reversal at small voltage, or the spin-rectification effect, has been rare.

In order to realize the spin-rectification effect, in this work, we employed active band-alignment engineering in a spin valve structure consisting of molecular ferroelectric croconic acid ($C_5H_2O_5$ or CA) sandwiched between ferromagnetic electrodes $La_{0.7}Sr_{0.3}MnO_3$ (LSMO) and Co. The advantage of CA [Fig. 1(b)] is its large electric polarization (25 $\mu C/cm^2$)[13] and unique proton-transfer origin of ferroelectricity[13–16], which enhances the electrostatic effect and minimizes the interfacial structural change. Using a poling voltage, the spin valve structure can be switched between a low-resistance (ON) state and a high-resistance (OFF) state in which the spin-rectification effect can be observed.

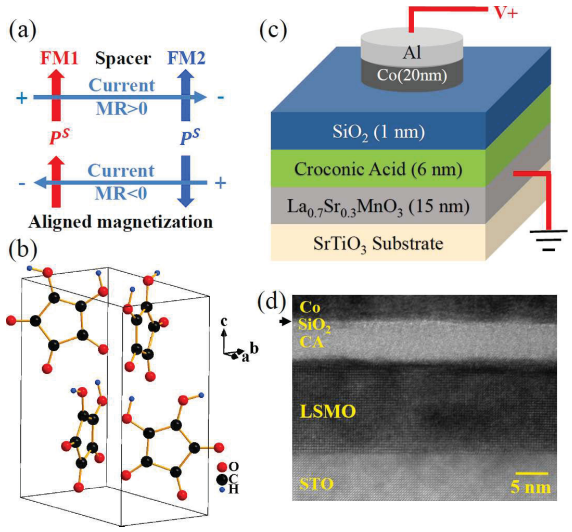

FIG. 1. (Color online) (a) Schematic illustration: upon current reversal, when the P^s sign of one FM/NM interface remains the same, MR sign reversal suggests P^s sign reversal or the spin-rectification effect of the other interface. (b) Crystal structure of CA, where the electrical polarization is along the c axis. (c) Schematics of the LSMO/CA/SiO_2/Co spin valve structure and its (d) HRTEM image.

The structure of the LSMO/CA/SiO_2/Co spin valve is schematically shown in Fig. 1(c) (see Fig. S1 in Supplementary Material[17]). A 15 nm thick LSMO layer was first epitaxially grown on the $SrTiO_3$ (001) substrate, where the 0.7/0.3 composition is chosen for its robust magnetic properties[18]. A 6 nm CA film was then evaporated on the LSMO surface as the spacer, followed by a SiO_2 layer

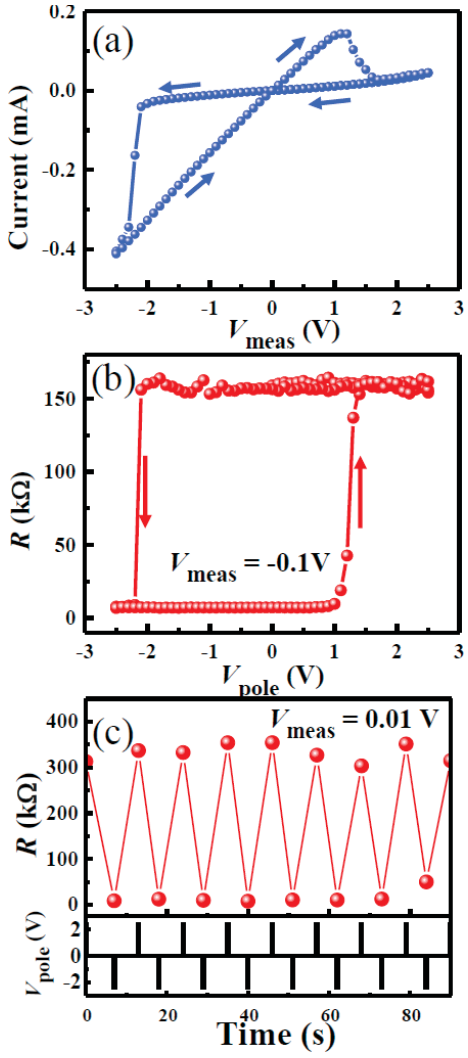

FIG. 2. (Color online) (a) Current versus voltage (V_{meas}) characteristics. (b) Resistances as a function of V_{pole} measured at V_{meas} = -0.1 V. (c) The typical resistance switching between the ON and OFF states measured at V_{meas} = -0.1V, after applying V_{pole} of +2.5V or -2.5V. The measurements were carried out at 30 K.

(≈1 nm) on the CA film as a diffusion barrier. The Co (20 nm)/Al (2 nm) top electrode with a diameter of ≈200 μm was grown using e-beam evaporation with a shadow mask. The growth of CA, SiO_2, Co, and Al layers was carried out at -30 °C substrate temperature to optimize the CA layer morphology and to minimize the inter-layer diffusion[19]. Figure 1(d) shows a high-resolution transmission electron microscopy (HRTEM) image from an as-grown LSMO/CA/SiO_2/Co heterostructure, confirming the epitaxy of LSMO and the desired thicknesses of different layers. Polarization hysteresis loop measurements and piezoresponse force microscopy were used to characterize the ferroelectric properties of the CA film, as demonstrated by our previous study[19].

As indicated by the structure in Fig. 1(c), a voltage was applied to the Co top electrode, and the LSMO bottom electrode was always grounded. Figure 2(a) shows a typical current-voltage (I-V) characteristics measured at 30 K with a bipolar switching between a high-resistance (ON) state and a low-resistance (OFF) state. The weak temperature dependence of resistance suggests tunneling nature of the conduction (see Fig. S2 in Supplementary Material[17]). The electroresistance, defined as ER≡ R_{OFF}/R_{ON}, increases with decreasing V_{meas} and reaches 3500 % close to zero V_{meas} (see Fig. S2 in Supplementary Material[17]), where R_{OFF} and R_{ON} are the resistance for the OFF and ON states respectively.

To further demonstrate the ER behaviors, we applied a sequence (2.5V → -2.5 V → 2.5V) of pulsed (20 ms duration) poling voltage (V_{pole}) on the junction to change the resistance state which is measured at a constant V_{meas} = -0.1 V right after the pulse; the measured resistance as a function of V_{pole} is shown in Fig. 2(b). Consistent with the I-V measurement in Fig. 2(a), the junction shows low-resistance states after negative V_{pole} <-2.3 V and high-resistance states after positive V_{pole} >1.5 V. To confirm the reversible switching between the ON and OFF states, measurements were performed by applying +2.5 V and -2.5 V pulses back and forth; the reproducibility was demonstrated in Fig. 2(c).

Figure 3(a) and (b) show representative curves of resistance versus magnetic field $R(H)$ for the junction in the ON and OFF states. Typical $R(H)$ curves with rapid resistance change at the coercive fields of LSMO and Co electrodes were observed. Here, the switching at the smaller (larger) magnetic fields corresponds to the magnetization reversal in LSMO (Co) electrode, consistent with the magnetometry measurements (see Fig. S3 in Supplementary Material[17]).

The behavior of MR for the ON and OFF states differ dramatically; here MR ≡ $(R_{AP} - R_P)/R_P$ where R_P and R_{AP} are the resistance when the magnetization of the FM electrodes are parallel and antiparallel respectively. In the ON state, MR is negative at both V_{meas} =-1 and 1 V, as shown in Fig. 3(a) and 3(b) respectively. Voltage dependence of MR, i.e. MR(V_{meas}), is shown in Fig. 3(c); negative MR has been observed regardless of the sign of V_{meas} in the ON state. This is typical for magnetic tunnel junctions using two ferromagnetic electrodes with opposite P^s[20,21]. The magnitude of MR, up to 12.5 %, decreases with increasing $|V_{meas}|$ in the ON state, consistent with mechanism of spin depolarization of hot electrons[12]. In contrast, in the OFF state, MR at V_{meas} =-1 and 1 V has opposite sign, as shown in Fig. 3(a) and 3(b) respectively. In fact, as shown in Fig. 3(c), MR is essentially positive at negative V_{meas} and negative at positive V_{meas} with a 0.1 V offset in the OFF state. This is different from the V_{meas}-independent MR sign in previously reported organic spin valve[22].

The dramatic difference between MR(V_{meas}) of the ON and OFF states was also observed at higher temperatures, e.g. 100 K (see Fig. S4 in Supplementary Material[17]). In the OFF state, the MR sign reverses at around V_{meas}=-0.1 V which is similar to that at 30 K,

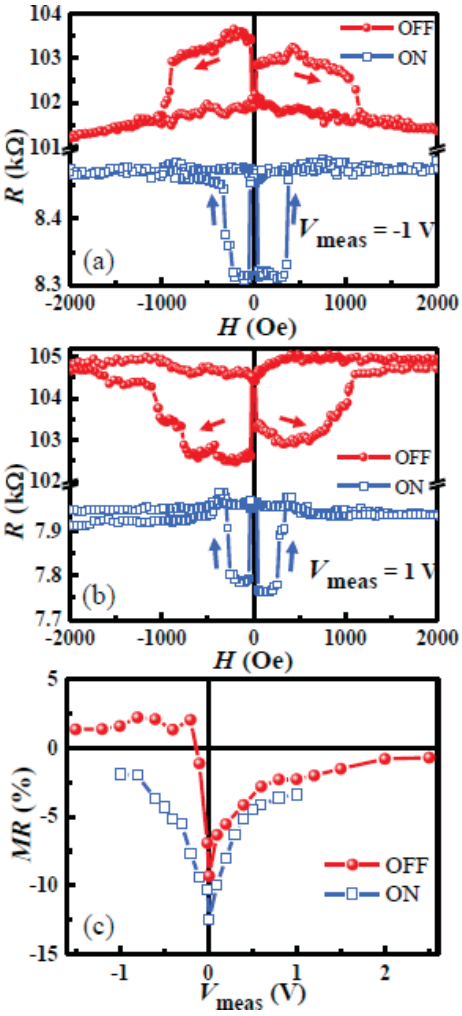

FIG. 3. (Color online) MR under (a) V_{meas} = -1 V and (b) V_{meas} = +1V after applying V_{pole} = +2.5 V and V_{pole} = 2.5 V respectively. The arrows indicate the measurement sequence. (c) MR as a function of V_{meas} for both ON (low resistance) and OFF (high resistance) states. The measurements were carried out at 30 K, with an in-plane magnetic field.

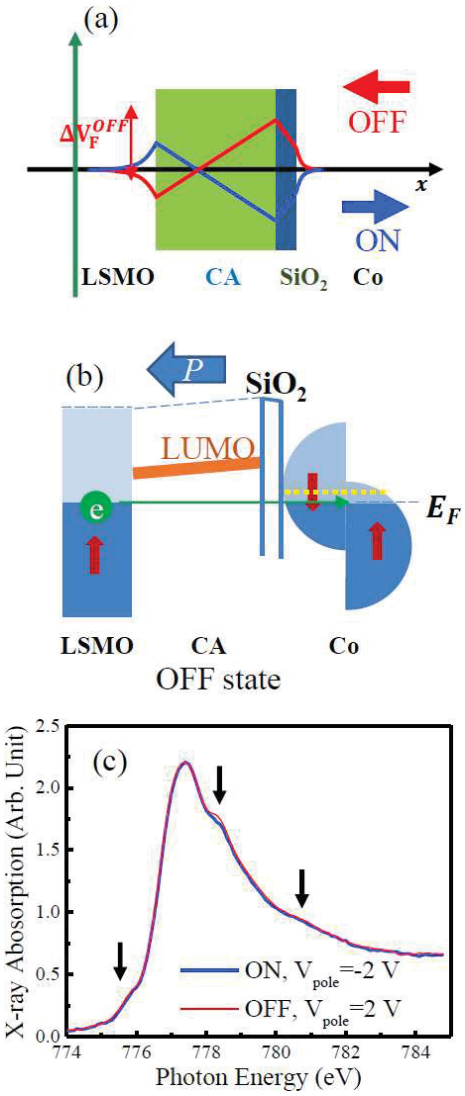

FIG. 4. (Color online) (a) Schematics of the electronic vacuum potential for both the ON and OFF states; the arrows indicate polarization direction of CA. ΔV_F^{OFF} is the change of vacuum potential in the ferroelectric layer in the OFF state. (b) Energy diagram illustrating the shift of Fermi energy in interfacial Co at zero measurement bias voltage due to the electrostatic effect in the OFF states. The vertical thick arrows indicate magnetization directions. The horizontal green arrows indicate the tunneling process. The yellow dashed lines indicate the bulk Fermi energy level of Co. (c) X-ray absorption spectra of the Co L_3 edge for the ON and OFF states. The arrows indicate features from Co^{2+}. The measurements were carried out at 80 K.

while in the ON state, the MR sign is also always negative with a peak value about -9.1%.

The direct effect of V_{pole} on the resistance of the junction, i.e. ER, can be understood with the mechanism of tunnel ferroelectric resistance, which was predicted theoretically in $SrRuO_3/BaTiO_3/SrTiO_3/SrRuO_3$ heterojunction[23]. The surface charge σ_P of a ferroelectric layer sandwiched between electrodes is normally screened at the ferroelectric/electrode interfaces. More specifically, at short-circuit condition, the screening charge is $\sigma_S = \sigma_P d_F/(\delta_1 + \delta_2 + d_F)$, where d_F is the thickness of the ferroelectric layer, δ_1 and δ_2 are the screening lengths of the two electrodes[24]. When $\delta_1+\delta_2 << d_F$, which is the case for typical metals, σ_S approaches σ_P, meaning a complete screening. The change of vacuum potential in the ferroelectric layer can be written as $\Delta V_F = d_F(\sigma_P - \sigma_S)/\varepsilon_0$[24], which vanishes when σ_S approaches σ_P, where ε_0 is the vacuum permittivity. With the dielectric layer SiO_2 inserted, the screening charge follows $\sigma_S = \sigma_P d_F/(\delta_1 + \delta_2 + d_F + d_D/\varepsilon_D)$, where d_D and ε_D are the thickness and the relative dielectric constant of the SiO_2 layer. If $\delta_1 + \delta_2 + d_D/\varepsilon_D$ is comparable to d_F, σ_S is substantially reduced and ΔV_F becomes nonzero. The change of vacuum potential affects the energy landscape of the tunnel junction and

most importantly the effective height of the tunnel barrier. As illustrated in Fig. 4(a) (see also Fig. S6 and Fig. S7 in Supplementary Material[17]), the overall vacuum level shifts up (down) when the CA polarization points down (up) towards LSMO (Co), which is expected to raise (lower) the tunnel barrier and cause higher (lower) resistance; this is consistent with the observation in the LSMO/CA/SiO_2/Co junction [Fig. 2]: positive (negative) poling voltage leads to the OFF (ON) state.

To understand the effect of V_{pole} on MR(V_{meas}), we first notice that MR(V_{meas}) depends on the energy landscape of the LSMO/CA/SiO_2/Co junction. For spin-conserved tunneling across the junction, according to the Jullieres model[25], the sign of the MR is determined by the product $P^s_{LSMO}P^s_{Co}$. Previous work demonstrated that, in a LSMO/$SrTiO_3$/Co spin valve, the energy and spin polarization of electrons participating in the charge transfer depend on V_{meas}, causing the dependence of effective P^s and MR on V_{meas} and even a MR sign change[20,21]. While the spin polarizations of the LSMO interface (P^s_{LSMO}) is believed to remain positive around the Fermi level due to the large gap between the Fermi energy and the minority band[18,26,27], the spin polarizations of the Co interface (P^s_{Co}) changes dramatically with energy (see Fig. S8 in Supplementary Material[17]). So, it was concluded that the MR(V_{meas}) relation in the LSMO/$SrTiO_3$/Co spin valve came mostly from the dependence of P^s_{Co} on V_{meas}[20,21]; Unfortunately, the V_{meas} needed for the MR sign change is too large (≈1 V). In contrast, in this work, in the OFF state of the LSMO/CA/SiO_2/Co junction, the MR sign reversal occurs at much smaller V_{meas} (≈ 0.1 V). Therefore, assuming that the P^s_{LSMO} sign remains the same, in the OFF state of LSMO/CA/SiO_2/Co spin valve reported here, P^s_{Co} basically changes sign when V_{meas} changes sign, i.e., the Co interface exhibits the spin-rectification effect, as illustrated in Fig. 1(a).

Following the mechanism of spin-conserved tunneling[20,21], if the Fermi energy of Co is shifted relative to the density of states, the MR(V_{meas}) relation will be shifted accordingly. In particular, to have a sign change of MR around zero V_{meas} in the OFF state, it is required that the P^s_{Co} reverses sign around the Fermi energy, which means a downshift of the Fermi energy relative to the density of states since the minority spin dominates at the Fermi energy in bulk Co. The measured $R(H)$ relation [Figs. 3(a) and (b)] indicates that the coercivity of the Co is clearly larger (smaller) when the junction is in the OFF (ON) state, suggesting a change of electronic structure. In contrast, the magnetic hysteresis loop of Co measured using a local X-ray magnetic circular dichroism (XMCD) probe, show less obvious change between the ON and OFF states (see Fig. S9 in Supplementary Material[17]), suggesting the change occurs at the interface. Here we propose that the downshift of Fermi energy relative to the density of state for the interfacial Co in the OFF state, is caused by the electrostatic effect of the ferroelectric polarization, as illustrated in Fig. 4(b) (see Fig. S10 in Supplementary Material[17]).

As depicted in Fig. 4(b), the electric polarization of a ferroelectric material may shift the vacuum potential across the junction. At open circuit condition, this vacuum-potential shift causes the shift of density of states of Co. At short-circuit condition (zero V_{meas}), to unify the Fermi energy of the whole junction, a charge accumulation/depletion and a shift of Fermi energy relative to the density of states in the interfacial Co occurs. For example, as illustrated in Fig. 4(b), in the OFF state, the polarization pointing toward LSMO causes electron depletion in Co, raises its density of states, and downshift its Fermi energy at zero V_{meas} (see Fig. S10 in Supplementary Material[17]). The order of magnitude of the energy shift can be estimated using $\Phi = \sigma_S\delta/\varepsilon_0 \approx \sigma_P\delta/\varepsilon_0 \sim 1$ V (see Section S4 in Supplementary Material[17]), where $\sigma_P \sim 10\ \mu C/cm^2$ and $\delta \sim 1$ Å are assumed; this is in reasonable agreement with the expected energy shift considering the V_{meas} (≈1 V) needed for the MR sign change in the LSMO/STO/Co junction reported previously[20,21].

To confirm possible depletion of electron in Co for the OFF state, we carried out X-ray absorption spectroscopy study on the Co L edge at 80 K. As shown in Fig. 4(c), the depletion of electron in Co for the OFF state relative to that for the ON state has been observed: the spectra of Co in the OFF state show a larger signature of Co^{2+} than that of the ON state[28] (see Fig. S9 in Supplementary Material[17]).

The proposed explanation above is based on the electronstatic effect of ferroelectric interface on spin transport[29–33]. The ferroelectric interface can significantly impact the spin transport by altering interfacial crystal and electronic structures[22,34–40], or by changing the energy-band alignment due to the electrostatic effect of the polarization[24,31,41,42]. Due to the weak organic/inorganic interaction, the electrostatic effect is expected to be more important in spin valves with organic ferroelectric spacers. Following this idea, spin valves with an organic ferroelectric spacer poly(vinylidene fluoride) (PVDF) was previously studied in LSMO/PVDF/Co junctions[22]. However, instead of the electrostatic effect, the significant change of interfacial structure of PVDF from H termination to F termination due to the rotation of polymer chains, was found to cause the change of interfacial spin polarization after the ferroelectric polarization reversal.[22] The idea of minimizing the structural effect at the ferroelectric interface, was previously examined in LSMO/PZT/Alq_3/Co spin-valves, where Alq_3, short for tris-(8-hydroxyquinoline) aluminum[31], was inserted between the ferroelectric spacer PZT and the magnetic electrode Co. On the other hand, in this structure, a large shift of Co interfacial Fermi energy relative to its density of state is not expected, because Co is separated from PZT by a thick (≈50 nm) Alq_3 layer.

The benefit of using organic ferroelectric CA is that its small interfacial structural change and large electric

polarization (25 μC/cm^2)[13] due to the proton-transfer origin of ferroelectricity[13–16], plus the weak interactions at the organic/inorganic interfaces, is expected to minimize structural effect and promote the electrostatic effect. The results of this work indeed provide evidence of the voltage-controlled energy-band alignment, which is the expected electrostatic effect of the polarization reversal.

We note that it is also possible that downshift of Fermi energy relative to the density of state for the interfacial Co in the OFF state of the junction is caused by the redox effect of Co (see Fig. S11 in Supplementary Material[17]). In principle, the oxygen vacancy (V_O^+) in SiO_2 may migrate when the poling voltage (V_{pole}) is applied. The ON state results from a negative V_{pole}, which moves oxygen vacancy toward Co and reduces Co. In contrast, the OFF state results from a positive V_{pole}, which moves oxygen vacancy away from Co and causes oxidation of Co at the interface. In the OFF state, the interfacial Co layer may be viewed as depleted with electron; correspondingly the Fermi energy is shifted downwards, which may shift the MR(V_{meas}) relation and causes reversal of MR sign around zero V_{meas}.

Whether the Fermi energy shift is caused by the ferroelectric electrostatic effect or by the Co redox effect, it appears that the energy landscape engineering is the key to tune the interfacial spin polarization P^s. This mechanism appears to be a viable route to adjust MR(V_{meas}) to generate the spin-rectification effect, which could be crucial for designing spintronics devices, similar to the role of charge-current rectification in modern semiconductor electronics.

In summary, we demonstrate the voltage control of the spin transport in the LSMO/CA/SiO_2/Co spin valves. Both ER effect and MR effect were obtained, and the MR sign could be tuned not only by the poling voltage but also by the measurement voltage. The MR (V_{meas}) relation in the OFF state suggests the spin-rectification effect at the Co interface. These observations are consistent with the mechanism of voltage-tunable interfacial energy-band alignment that may result from the electrostatic effect of the ferroelectric polarization or the redox effect of Co electrode. These results suggest the importance of energy-band alignment in spin transport across spin valves, confirm the advantage of organic spintronics using a molecular semiconductor as the barrier in spin valves, and reveal an intriguing spin-rectification behavior which is promising for functionalities.

Research primarily supported by the U.S. Department of Energy (DOE), Office of Science, Basic Energy Sciences (BES), under Award # DE-SC0019173 (device fabrication, transport measurements, magnetometry, X-ray spectroscopy, and modeling). Additional support are from the National Science Foundation (NSF) through the Nebraska Materials Research Science and Engineering Center under DMR-1420645 (electron microscopy), NSF DMR-1710461 (oxide film growth), NSFC-51790491 and NKRDPC-2019YFA0307900 (data analysis, manuscript drafting/revision). Use of the Advanced Light Source was supported by the U.S. Department of Energy, Office of Science, Office of Basic Energy Sciences under Contract No. DE-AC02-05CH11231. The research was performed in part in the Nebraska Nanoscale Facility: National Nanotechnology Coordinated Infrastructure and the Nebraska Center for Materials and Nanoscience, which are supported by the National Science Foundation under Grant No. ECCS-1542182, and the Nebraska Research Initiative.

[1] J. Sinova, S. O. Valenzuela, J. Wunderlich, C. H. Back, and T. Jungwirth, Rev. Mod. Phys. 87, 1213 (2015).
[2] I. uti, J. Fabian, and S. Das Sarma, Rev. Mod. Phys. 76, 323 (2004).
[3] J. Wunderlich, B.-G. Park, A. C. Irvine, L. P. Zarbo, E. Rozkotova, P. Nemec, V. Novak, J. Sinova, and T. Jungwirth, Science (80-.). 330, 1801 (2010).
[4] S. Sanvito, Nat. Phys. 6, 562 (2010).
[5] Z. H. Xiong, D. Wu, Z. Valy Vardeny, and J. Shi, Nature 427, 821 (2004).
[6] [27] F. Wang and Z. V. Vardeny, J. Mater. Chem. 19, 1685 (2009).
[7] V. A. Dediu, L. E. Hueso, I. Bergenti, and C. Taliani, Nat. Mater. 8, 707 (2009).
[8] [26] F. Wang and Z. V. Vardeny, Synth. Met. 160, 210 (2010).
[9] R. Geng, T. T. Daugherty, K. Do, H. M. Luong, and T. D. Nguyen, J. Sci. Adv. Mater. Devices 1, 256 (2016).
[10] J. Devkota, R. Geng, R. C. Subedi, and T. D. Nguyen, Adv. Funct. Mater. 26, 3881 (2016).
[11] H.-J. Jang and C. A. Richter, Adv. Mater. 29, 1602739 (2017).
[12] S. O. Valenzuela, D. J. Monsma, C. M. Marcus, V. Narayanamurti, and M. Tinkham, Phys. Rev. Lett. 94, 196601 (2005).
[13] S. Horiuchi, Y. Tokunaga, G. Giovannetti, S. Picozzi, H. Itoh, R. Shimano, R. Kumai, and Y. Tokura, Nature 463, 789 (2010).
[14] S. Horiuchi, R. Kumai, and Y. Tokura, Adv. Mater. 23, 2098 (2011).
[15] S. Horiuchi, F. Kagawa, K. Hatahara, K. Kobayashi, R. Kumai, Y. Murakami, and Y. Tokura, Nat. Commun. 3, 1308 (2012).
[16] Y. Noda, T. Yamada, K. Kobayashi, R. Kumai, S. Horiuchi, F. Kagawa, and T. Hasegawa, Adv. Mater. 27, 6475 (2015).
[17] See Supplemental Material at [URL will be inserted by publisher] for experimental details, V_{meas}-dependent electroresistance (ER), magnetoresistance (MR), energy band structure, spin polarization and MR, X-ray absorption study on the Co electronic structure, mechanisms of shifting Fermi energy of Co.
[18] E. Dagotto, T. Hotta, and A. Moreo, Phys. Rep. 344, 1 (2001).

[19] X. Jiang, H. Lu, Y. Yin, X. Zhang, X. Wang, L. Yu, Z. Ahmadi, P. S. Costa, A. D. Dichiara, X. Cheng, A. Gruverman, A. Enders, and X. Xu, Appl. Phys. Lett. 109, 102902 (2016).

[20] J. De Teresa, A. Barthlmy, A. Fert, J. Contour, R. Lyonnet, F. Montaigne, P. Seneor, and A. Vaurs, Phys. Rev. Lett. 82, 4288 (1999).

[21] J. De Teresa, A. Barthelemy, A. Fert, J. P. Contour, F. Montaigne, P. Seneor, Science 286, 507 (1999).

[22] S. Liang, H. Yang, H. Yang, B. Tao, A. Djeffal, M. Chshiev, W. Huang, X. Li, A. Ferri, R. Desfeux, S. Mangin, D. Lacour, M. Hehn, O. Copie, K. Dumesnil, and Y. Lu, Adv. Mater. 28, 10204 (2016).

[23] J. P. Velev, J. D Burton, M. Y. Zhuravlev and E. Y. Tsymbal, npj Computational Materials 2, 16009 (2016).

[24] M. Y. Zhuravlev, R. F. Sabirianov, S. S. Jaswal, and E. Y. Tsymbal, Phys. Rev. Lett. 94, 246802 (2005).

[25] M. Julliere, Phys. Lett. A 54, 225 (1975).

[26] J.-H. Park, E. Vescovo, H.-J. Kim, C. Kwon, R. Ramesh, and T. Venkatesan, Phys. Rev. Lett. 81, 1953 (1998).

[27] J. Renard and A.-M. Haghiri-Gosnet, J. Phys. D. Appl. Phys. 36, R127 (2003).

[28] S. S. Lee, J. H. Kim, S. C. Wi, G. Kim, J. S. Kang, Y. J. Shin, S. W. Han, K. H. Kim, H. J. Song, and H. J. Shin, J. Appl. Phys. 97, 10A309 (2005).

[29] V. Garcia, M. Bibes, L. Bocher, S. Valencia, F. Kronast, A. Crassous, X. Moya, S. Enouz-Vedrenne, A. Gloter, D. Imhoff, C. Deranlot, N. D. Mathur, S. Fusil, K. Bouzehouane, and A. Barthelemy, Science 327, 1106 (2010).

[30] D. Pantel, S. Goetze, D. Hesse, and M. Alexe, Nat. Mater. 11, 289 (2012).

[31] D. Sun, M. Fang, X. Xu, L. Jiang, H. Guo, Y. Wang, W. Yang, L. Yin, P. C. Snijders, T. Z. Ward, Z. Gai, X.-G. Zhang, H. N. Lee, and J. Shen, Nat. Commun. 5, 4396 (2014).

[32] R. C. Subedi, R. Geng, H. M. Luong, W. Huang, X. Li, L. A. Hornak, and T. D. Nguyen, Appl. Phys. Lett. 110, 053302 (2017).

[33] A. Rajapitamahuni, L. L. Tao, Y. Hao, J. Song, X. Xu, E. Y. Tsymbal, and X. Hong, Phys. Rev. Mater. 3, 021401(R) (2019).

[34] J. M. Lpez-Encarnacin, J. D. Burton, E. Y. Tsymbal, and J. P. Velev, Nano Lett. 11, 599 (2011).

[35] S. Valencia, A. Crassous, L. Bocher, V. Garcia, X. Moya, R. O. Cherifi, C. Deranlot, K. Bouzehouane, S. Fusil, A. Zobelli, A. Gloter, N. D. Mathur, A. Gaupp, R. Abrudan, F. Radu, A. Barthlmy, and M. Bibes, Nat. Mater. 10, 753 (2011).

[36] J. P. Velev, J. M. Lopez-Encarnacion, J. D. Burton, and E. Y. Tsymbal, Phys. Rev. B 85, 125103 (2012).

[37] T. L. Meyer, A. Herklotz, V. Lauter, J. W. Freeland, J. Nichols, E. J. Guo, S. Lee, T. Z. Ward, N. Balke, S. V. Kalinin, M. R. Fitzsimmons, and H. N. Lee, Phys. Rev. B 94, 174432 (2016).

[38] J. D. Burton and E. Y. Tsymbal, Phys. Rev. B 80, 174406 (2009).

[39] X. Hong, A. Posadas, A. Lin, and C. H. Ahn, Phys. Rev. B 68, 134415 (2003).

[40] J. Heidler, M. Fechner, R. V. Chopdekar, C. Piamonteze, J. Dreiser, C. A. Jenkins, E. Arenholz, S. Rusponi, H. Brune, N. A. Spaldin, and F. Nolting, Phys. Rev. B 94, 014401 (2016).

[41] M. Y. Zhuravlev, S. S. Jaswal, E. Y. Tsymbal, and R. F. Sabirianov, Appl. Phys. Lett. 87, 222114 (2005).

[42] X. Xu, J. Mater. 4, 1 (2018).